The Aqueous Viscous Drag of a Contracting Open Surface

Fredric S. Cohen* and Rolf J. Ryham†

May 9, 2013

Abstract

A problem for fluid flow around an axisymmetric spherical surface with a hole is presented to characterize pore dynamics in liposomes. A rotational stream function for the contraction of a punctured plane region is obtained and is used in the perturbation expansion for a stream function in the case of a spherical surface with a hole of small radius compared to the spherical radius. The Rayleigh dissipation function is calculated and used to infer the aqueous friction induced by the contraction of the hole. The theoretical aqueous friction coefficient is compared with one derived from experimental data, and they are in agreement.

1 Introduction

Biological membranes consist of lipids and proteins. Membranes deform as a natural part of many biological processes, such as the changes in shape red blood cells undergo as they pass through capillaries, the merger of separate membranes in the release of neurotransmitters

*Rush University Medical Center, Department of Molecular Biophysics and Physiology, 1750 W Harrison St, Chicago, IL 60612, (Fredric_Cohen@rush.edu).

†Fordham University, Department of Mathematics, 441 E. Fordham Road, Bronx, NY 10458, (rryham@fordham.edu).

in the brain, and the engulfment of large extracellular molecules by cells. The deformation of membranes is hindered by the internal viscosity of the membrane and by the aqueous viscosity of the surrounding water.

A single bilayer can be arranged into a sphere that separates interior and exterior aqueous compartments. These liposomes can be large (20 μm), mimicking cell membranes, or small (100 nm), modeling membranes of intracellular granules. Pores more or less circular, form in membranes as a result of injury of osmotic bursting and the spherically shaped membrane surface becomes open to the extracellular solution. Pore dynamics has been experimentally modeled by osmotic swelling of liposomes, and it has been found that the pore grows until the internal pressure of the liposome, responsible for swelling, is relieved; the hole then shrinks, minimizing its circumference.

The standard theory that had been used to predict pore growth and shrinkage assumed that dissipation of the energy stored within the stretched bilayer is dominated by the viscosity of the bilayer itself [2]. This prior theory, however, did not correctly account for pore dynamics as a function of aqueous viscosity; the time course for growth and shrinkage of the pore is slowed as the aqueous viscosity is experimentally increased, and the prior theory ignored any contribution of aqueous viscosity to energy dissipation [2, 16]. More recently we developed a theory that does properly describe the experimentally observed dependence. We further showed by dimensional analysis that aqueous viscosity, and not bilayer viscosity, is the leading term in the dissipation function [20]. But this recent theory assumed that the bilayer was flat, whereas liposomes and cells are spherical. A drag friction coefficient accounting for the aqueous viscosity was obtained empirically by fitting this theory to experimental data of measured pore time courses.

In this note, we present a self contained theoretical derivation for the viscous drag of the ambient fluid for spherical, rather than flat, open membranes. We will refer to the viscous drag as *aqueous friction*. We view a liposome with a pore as an axisymmetric, two dimensional surface immersed in an incompressible, viscous, Newtonian fluid. We present a boundary value problem for the fluid flow around the surface. In the biological situation,

the Reynolds number $\mathrm{Re} = \rho U L/\mu \approx 10^{-5}$ is low; the velocity is obtained from a stream formulation for the equations of motion. We first study the case of a sphere with infinite radius and obtain a closed form solution for the stream function around a flat plane with a hole. We address the case of a sphere with finite radius by using the method of perturbation expansion assuming the ratio between the radius of the hole and the radius of the sphere is small. We then calculate the rate of mechanical energy dissipation in order to infer the following value of the aqueous friction coefficient;

$$\gamma(\epsilon) = 2\pi - 4\epsilon \ln \frac{\epsilon}{2} + \cdots \tag{1}$$

where ϵ is the non-dimensional ratio of hole radius to sphere radius. Equation 1 shows that the friction coefficient for a contracting, infinite, flat plane with a hole is precisely 2π. This coefficient increases as the plane is made spherical with a finite radius that is large when compared to the radius of the hole. We combine the value of $\gamma(\epsilon)$, which now depends on the liposome geometry, with the Raleigh dissipation equation to derive pore dynamics.

The analytical and numerical calculation of the interaction between fluid flows and bounding regions is in general a difficult problem that is further complicated by the domain geometry. The boundary integral [17, 25, 27], immersed boundary [14, 15], and phase field [21] methods are three important numerical methods capable of modeling these interactions. Exact expressions for the fluid flow, like those obtained by [9] for the nonlinear flow over a spreading, flat surface, are rare. For the annular region we consider in this note, [5] obtained the shear forces for unidirectional flow across the circular hole in a plane wall. Exact solutions for the Stokes flow and drag force for a spherical cap in a uniform far field flow have been derived [8, 18]. In these works, the steady streaming flow describes the rigid translation of a spherical cap in a viscous fluid at rest. The velocity is constant on the boundary. In contrast, in the present study the streaming flow is unsteady and the spherical cap is not rigid, but rather can contract or expand. The magnitude and direction of the velocity on the boundary depend on both position and time. The consequences of viscous drag on oscillating cantilevers used for atomic force microscopes has also been considered through a shape dependent hydrodynamic function [22]. There has been significant work that has

considered the retraction of viscous sheets that is controlled by energy dissipation internal to the bilayer itself, but ignoring any contributions caused by movement of the ambient viscous fluid [1, 4, 6, 7, 24]. To our knowledge a closed form expression for the stream function accounting for the interaction between a spreading surface that contains a circular hole with the viscous ambient medium has not been described before.

In the next Section, we present the stream function formulation for axisymmetric Stokes flow and derive particular solution expansions of the stream equation. In Section 4, we solve the flow problem for the contraction of a flat plane surface. In Section 5, we solve the analogous flow problem for a spherical surface using the method of perturbation expansions. The dissipation function and the friction coefficient given by Equation 1 are calculated at the ends of Sections 4 and 5. The results of these calculations are compared in Section 6 with the numerical value of the aqueous friction coefficient obtained by empirical means. An experiment that would explicitly test our theory is suggested.

2 Acknowledgement

We would like to thank Darren Crowdy and for helpful suggestions in the preparation of this manuscript and the referees for pointing out valuable comparisons. F.S.C. is supported by NIHR01 GM066837.

3 Notation and Preliminaries

We treat the problem of determining the flow field in the aqueous region surrounding the membrane by the method of the Stokes' stream function. Consider an axisymmetric, open surface Σ_t with a single hole where the surface is moving with normal velocity v_n and tangential velocity v_s (Figure 1). The stream function ψ is a solution to the boundary value problem ([11]; 4-7.13)

$$D^2\psi - \frac{1}{\nu}(D\psi)_t = 0, \qquad x \in \mathbb{R}^3 \setminus \Sigma_t, \tag{2}$$

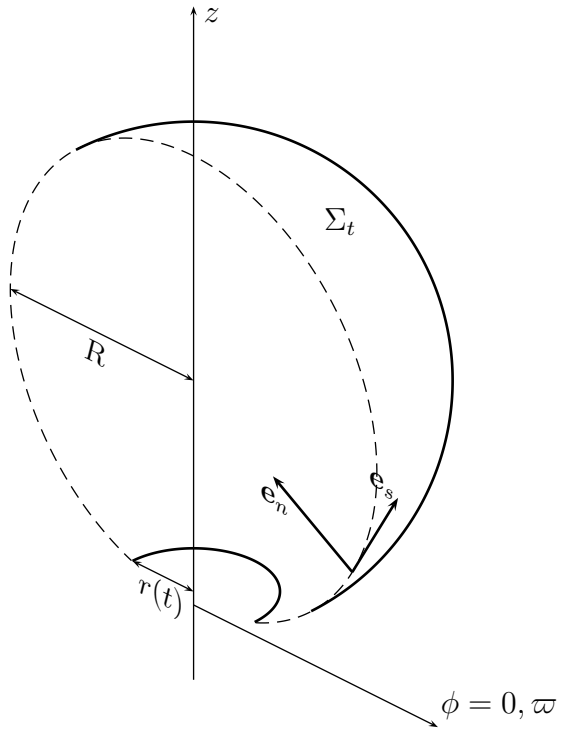

Figure 1: Cut-away portion of a rotationally symmetric open surface Σ_t representing a spherical liposome of radius R with a pore of radius $r(t)$ lying between the azimuthal angles $0 < \phi < \pi$. A viscous ambient fluid occupies the region bathing the surface.

$$\frac{1}{\varpi}\frac{\partial \psi}{\partial s} = -v_n, \quad x \in \Sigma_t, \tag{3}$$

$$\frac{1}{\varpi}\frac{\partial \psi}{\partial n} = v_s, \quad x \in \Sigma_t, \tag{4}$$

$$\psi = 0, \quad \varpi = 0. \tag{5}$$

Here, D is the stream operator which, in cylindrical coordinates (ϖ, z), reads

$$D = \frac{\partial^2}{\partial \varpi^2} - \frac{1}{\varpi}\frac{\partial}{\partial \varpi} + \frac{\partial^2}{\partial z^2}.$$

When $D\psi = 0$ the stream function ψ is said to be irrotational and when $D\psi \neq 0$ the stream function ψ is said to be rotational. Here $\nu = \mu/\rho$ is the kinematic viscosity where μ is the aqueous (dynamic) viscosity and ρ the aqueous density. The surface tangent $\mathbf{e}_s$ is oriented away from the hole and the surface normal $\mathbf{e}_n$ is chosen so that $(\mathbf{e}_s, \mathbf{e}_n)$ form a right-handed

orthonormal frame (Figure 1). In (3), the partial derivative of ψ is taken in the $\mathbf{e}_s$ direction with arc-length parameter s and in (4) the partial derivative of ψ is taken in the direction $\mathbf{e}_n$. Since Σ_t faces the fluid on two sides, we will distinguish the side of Σ_t lying in the direction $\mathbf{e}_n$ as positive and the side of Σ_t lying in the direction $-\mathbf{e}_n$ side as negative. Finally, (5) is the requirement that fluid flux be nonsingular on the axis of symmetry.

We will focus our attention on contractile motions of the Σ_t. As defined below, contraction is related to a dimensional parameter $r(t)$—the hole radius. Lipid bilayers are generally homogeneous so we let the lipid density be spatially constant. Mass conservation then implies that $\mathrm{div}_S\,\mathbf{v} = \frac{\partial \mathbf{v}}{\partial s}\cdot\mathbf{e}_s + \frac{1}{\varpi}\mathbf{v}\cdot\mathbf{e}_\varpi$ is independent of s, where $\mathbf{v} = v_s\mathbf{e}_s + v_n\mathbf{e}_n$ is the velocity of Σ_t, div_S is the surface divergence, and $\mathbf{e}_\varpi$ and $\mathbf{e}_z$ are the cylindrical basis vectors. If $v_n = 0$, then

$$v_s(s) = \frac{c_1}{\varpi} + \frac{c_2}{\varpi}\int_0^s \varpi\, du \tag{6}$$

where c_1 and c_2 are integration constants determined by the rim and far field tangential velocities.

In classical calculations, the drag force that is imposed on obstacles in a Stokes flow generally shares the same direction as the far field flow. In the present problem, this identification is not possible because the shear forces caused by contraction are radial. Strictly speaking, the total shear force is a pseudo force. We calculate the rate of mechanical energy dissipation as a function of μ, $r(t)$ and r' to infer the friction coefficient. Once $\mathbf{v}$ has been specified and the stream function ψ determined from (2-5) we calculate the Rayleigh dissipation function ([11]; 2-2.1, 4-14.10);

$$\Delta_{\mathrm{a}} = -2\mu\int_{\Sigma_t}\frac{v_s}{\varpi}D\psi\, dA. \tag{7}$$

The dissipation function Δ_{a} is the rate at which internal energy is transferred from the bilayer into the aqueous surrounding by viscous losses. The coefficient 2 preceding the previous integral accounts for the dissipation on the positive and negative side of Σ_t. We have also chosen a sign convention making Δ_{a} nonnegative.

To illustrate how the friction coefficient is derived from the dissipation function and applied to the problem of pore dynamics, let $E(r, R)$ be the internal energy of a liposome

as a function of the hole radius r and sphere radius R. For a liposome in which the internal pressure is zero, for example,

$$E(r,R) = T2\pi r + S\frac{(4\pi R^2 - 2\pi R r^2)}{8\pi R^2}$$

is the sum of the edge energy and stretching energy where $T = 2.5$ kT nm^{-1} is edge tension of a hole in a bilayer and $S = 0.045$ kT nm^{-2} is the modulus for unfolding of the wrinkles in the bilayer. The Rayleigh dissipation equation permits us to determine an evolution equation for $r(t)$;

$$\frac{1}{2}\frac{\partial \Delta}{\partial r'} = -\frac{\partial E}{\partial r} \tag{8}$$

where $\Delta = \Delta_{\rm a} + \Delta_{\rm m}$ and $\Delta_{\rm m}$ is the rate of internal energy dissipation due to viscous losses within the membrane. The aqueous friction coefficient γ is defined by the relation $\mathscr{F}_{\rm a} = 2\pi r r'\gamma$ where $\mathscr{F}_{\rm a} = \frac{1}{2}\frac{\partial \Delta_{\rm a}}{\partial r'}$ is the aqueous friction.

We study surfaces Σ_t which can be approximated by an infinite, flat plane punctured by a hole of radius $r(t)$ centered on the axis of symmetry;

$$\Sigma_t^0 = \{(\varpi, z, \phi) : \varpi > r(t), z = 0, 0 \le \phi < 2\pi\}.$$

Here, ϕ is the azimuthal angle. Solutions of (2-5) will be developed by the method of perturbation expansion ([26]) where we tentatively assume

$$\psi = \psi^0 + \epsilon\psi^1 + \cdots \tag{9}$$

and where ϵ is a small, non dimensional perturbation parameter. The stream functions in (9) are solutions to auxiliary boundary value problems on $\mathbb{R}^3 \setminus \Sigma_t^0$. The boundary data for ψ^0, ψ^1, ... are determined by the surface velocity, the coordinate changes associated with the approximation of Σ_t by Σ_t^0, and by any preceding terms in the expansion. We will restrict our attention to the first two terms in the expansion (9), although it is in principle possible to pursue terms of arbitrarily high order.

Following the method of [23], solutions to (2-5) are presented in oblate spheroidal coordinates

$$\varpi + iz = c\sinh(\xi + i\eta).$$

The contours $\xi = \text{const.}$ and $\eta = \text{const.}$ form an orthogonal family of planetary spheroids and hyperboloids respectively. The succeeding expressions will be simplified by working with the separable coordinates

$$p = \cos\eta, \quad q = \sinh\xi$$

for which

$$\varpi = r\sqrt{1-p^2}\sqrt{1+q^2}, \quad z = rpq. \tag{10}$$

In this way, the infinite cylinder $\{(p,q,\phi) : 0 < p < 1, -\infty < q < \infty, 0 \le \phi < 2\pi\}$ is conformally mapped onto the region $\mathbb{R}^3 \setminus \Sigma_t^0$. In these coordinates, the stream operator is

$$D = \frac{1}{r^2(p^2+q^2)}\left((1-p^2)\frac{\partial^2}{\partial p^2} + (1+q^2)\frac{\partial^2}{\partial q^2}\right).$$

Later in this note, rotational stream functions of the form

$$\psi_0 = qf(p), \quad \psi_1 = pg(p), \tag{11}$$

will arise for which $D^2\psi_0 = D^2\psi_1 = 0$ provided f and g are quadratic. Further solutions of the equation $D^2\psi = 0$ are obtained by the decomposition ([13])

$$\psi = \psi_{\text{irr}} + \psi_{\text{rot}}, \quad D\psi_{\text{irr}} = 0, \quad D\psi_{\text{rot}} = \omega, \quad D\omega = 0$$

where ψ_{irr} and ω are expressed in terms of Gegenbauer polynomials. Specifically,

$$\psi_{\text{irr},0} = 1, \quad \psi_{\text{irr},1} = p, \quad \psi_{\text{irr},2} = q, \quad \psi_{\text{irr},3} = pq, \quad \psi_{\text{irr},4} = \frac{1}{4}(p^2-1)(q^2+1), \quad \cdots \tag{12}$$

satisfy $D\psi_{\text{irr},n} = 0$ for $n = 0, 1, 2, \ldots$, and

$$\begin{aligned} &\psi_{\text{rot},0} = \frac{1}{2}(q^2 - p^2 + 2), \quad \psi_{\text{rot},1} = \frac{1}{2}q\left(\frac{1}{3}q^2 - p^2\right), \quad \psi_{\text{rot},2} = \frac{1}{2}p\left(q^2 - \frac{1}{3}p^2\right), \\ &\psi_{\text{rot},3} = \frac{1}{6}(pq^3 - p^3q + 2pq), \quad \cdots \end{aligned} \tag{13}$$

satisfy $D\psi_{\text{rot},n} = \psi_{\text{irr},n}$ for $n = 0, 1, 2, \ldots$. The mathematical details of the derivation of (12) and (13) are provided in the Appendix Section. We will determine the solution ψ to boundary value problems by setting

$$\psi = B\psi_0 + B'\psi_1 + \sum_{n=0}^{\infty} A_n\psi_{\text{irr},n} + \sum_{n=0}^{\infty} B_n\psi_{\text{rot},n} \tag{14}$$

where the value of the coefficients B, B', $A_0, A_1, \ldots,$ and $B_0, B_1, \ldots$ are chosen to satisfy the boundary conditions (3-5). [13] have obtained the general expansion the stream function in oblate spheroidal coordinates.

4 An Infinite, Flat Plane with Hole

As the base case, we consider the planar surface Σ_t^0 moving with tangential velocity

$$v_s(\varpi) = r' \frac{r}{\varpi} \tag{15}$$

and normal velocity

$$v_n(\varpi) = 0.$$

With this velocity, the rim of the hole contracts with rate r' and the area density is independent of position and t. This velocity is sometimes referred to as radial plug flow. It is immediately verified that v_s satisfies the continuity equation (6). Consider the associated boundary value problem

$$D^2\psi^0 - \frac{1}{\nu}(D\psi^0)_t = 0, \qquad x \in \mathbb{R}^3 \setminus \Sigma_t^0, \tag{16}$$

$$\frac{1}{\varpi}\frac{\partial \psi^0}{\partial \varpi} = 0, \qquad x \in \Sigma_t^0, \tag{17}$$

$$\frac{1}{\varpi}\frac{\partial \psi^0}{\partial z} = r' \frac{r}{\varpi}, \quad x \in \Sigma_t^0, \tag{18}$$

$$\psi^0 = 0, \qquad \varpi = 0. \tag{19}$$

With the help of (10), one verifies that the boundary conditions (17-19) imply

$$\psi^0(1, q) = 0, \quad \frac{\partial \psi^0}{\partial q}(0, q) = 0, \quad \frac{\partial \psi^0}{\partial p}(0, q) = r' r^2 q, \quad -\infty < q < \infty. \tag{20}$$

We therefore guess a solution of the form $\psi^0 = qf(p)$ given in (11). We require that $f(1) = 0, f(0) = 0$, and $f'(0) = r'r^2$. This is achieved by setting $f(p) = r'r^2 p(1-p)$ and therefore

$$\psi^0(p, q, t) = r'r^2(t) qp(1-p). \tag{21}$$

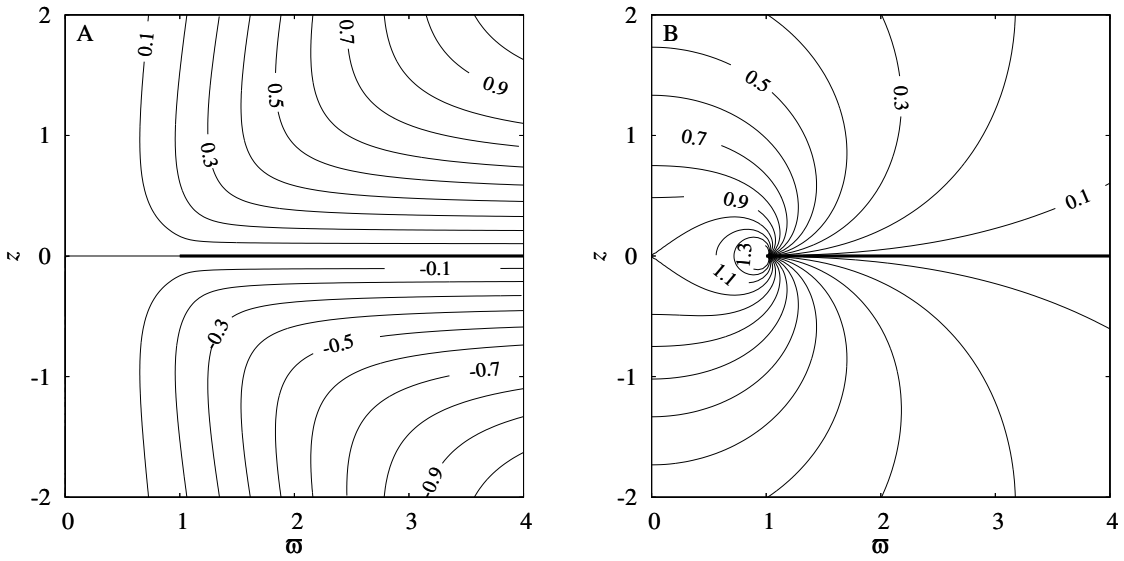

Figure 2: The contour lines of the stream function ψ^0/r' and values (panel A) and the contour lines of the pressure $\mathfrak{p}/2\mu r'$ and values (panel B) are both for the case $r = 1$. The surface Σ_t^0, depicted by the thick curve, represents a planar bilayer with a circular hole.

Note that ψ^0 is now also a solution of (16) because $D^2\psi^0 = 0$ and

$$D\psi^0 = \frac{-2r'q(1-p^2)}{p^2+q^2} \tag{22}$$

is independent of t, once terminal velocity is reached and r' is constant. The function ψ^0 is an exact solution to the unsteady Stokes flow problem for an incompressible plane region shrinking with constant speed around a circular hole.

The pressure $\mathfrak{p}$ can be integrated from the equations 4-26.1, 4-26.2, and 4-15.5 in [11], yielding

$$\mathfrak{p}(p,q,t) = -\frac{2\mu r' p}{r(t)(p^2+q^2)}. \tag{23}$$

Although the pressure $\mathfrak{p}$ is singular on the leading edge of the hole ($q = 0$), the dissipation of mechanical energy due to pressure vanishes. This occurs because the pressure is symmetric on opposite sides of Σ_t^0. Contours of the pressure and ψ^0 are provided by Figure 2. Although the velocity is an exact solution of the Stokes equation, it is not a solution to the full Navier-Stokes equations ($\nabla\psi^0 \times \nabla(\varpi^{-1}D\psi^0) \neq 0$). However, the very low Reynolds number implies

that the velocity fails to solve the full Navier-Stokes equation by a residual on the same order as the residual found in numerical approximations [10]; the linear Stokes flow is thus indistinguishable from the nonlinear flow in practical, biological applications.

The pressure field (23) in the vicinity of the pore edge is locally the same as the pressure field induced by the steady, two dimensional flow past a semi-infinite plate. Taking h to be the distance from a point in the plane with the surface, setting $p = 0$ in (23) and using (10), yields $\mathfrak{p} \sim -2r'\mu/r\sqrt{h}$. The expression $\tilde{\xi}\tilde{\eta}^2$ for the stream function in parabolic coordinates $(\tilde{\eta}, \tilde{\xi})$ at the leading edge of a flat plate is given by [3]. By integrating the equations of motion, the pressure on the leading edge of a flat plate $\mathfrak{p}_{\text{plate}}$ is then proportional to $\tilde{\eta}/(\tilde{\eta}^2 + \tilde{\xi}^2)$. Evaluating the pressure of the plate in the region adjacent to the edge gives $\mathfrak{p}_{\text{plate}}$ proportional to $1/\sqrt{h}$ which is locally of the same form as the pressure near the pore edge. A similar comparison holds for the flat plate and axisymmetric uniform flow past the leading edge of a hemispherical cup [8].

To evaluate the dissipation function, we set $p = 0$ in (10), (15), and (22), to find

$$\Delta_{\text{a}} = -2\mu \int_{\Sigma_t^0} \frac{v_s}{\varpi} D\psi \, dA = 8\pi\mu r(r')^2 \int_0^\infty \frac{1}{1+q^2} \, dq = 4\pi^2 \mu r(r')^2 \tag{24}$$

from which we infer

$$\mathscr{F}_{\text{a}} = 4\pi^2 \mu r r', \quad \gamma = 2\pi. \tag{25}$$

Here $\gamma = 2\pi$ is the leading term in the expansion (1). The succeeding terms in the expansion are calculated in the next section.

5 A Large Sphere with Hole

We use toroidal coordinates to model the spherical surface with a hole;

$$z + i\varpi = ir \coth \frac{\lambda + i\zeta}{2}.$$

The contours $\zeta =$ const. form a family of spheres centered on the axis of symmetry and λ parametrizes the circular arc extending from the axis of symmetry ($\lambda = 0$) to the point

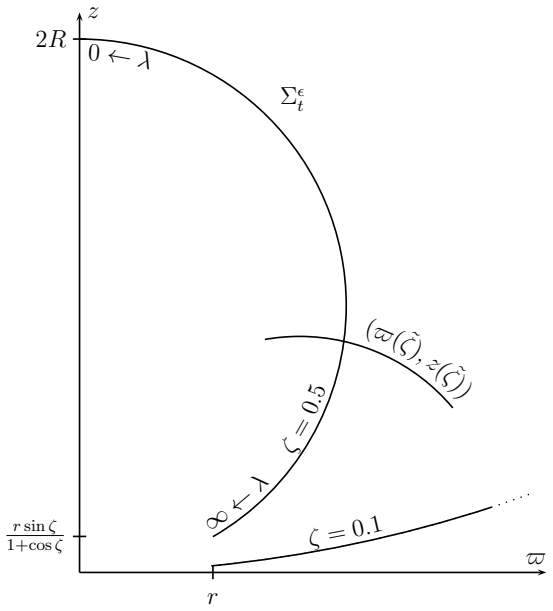

Figure 3: Toroidal coordinates parametrizing a large sphere Σ_t^ϵ with a hole of radius r. The ζ-contours form spheres of radius R; the z coordinate has been shifted up so that the base of the sphere passes through the origin. The curve $(\varpi(\tilde\zeta), z(\tilde\zeta))$ is orthogonal to the sphere. The pore rim and intersection with the axis of symmetry are parametrized by the limits $\lambda = \infty$ and $\lambda = 0$ respectively.

$(\varpi, z) = (r, 0)$ lying on the rim of the hole ($\lambda \to \infty$.) Let $R \gg r$, $\epsilon = \frac{r}{R}$, and define

$$\tilde\Sigma_t^\epsilon = \{(\varpi, z, \phi) : \sin\zeta = \epsilon\}.$$

Setting $\lambda = 0$ gives the value

$$\frac{r\sin\zeta}{1-\cos\zeta} + \frac{r\sin\zeta}{1+\cos\zeta} = \frac{2r}{\sin\zeta}, \quad (\text{with } \sin\zeta = \epsilon)$$

for the diameter of $\tilde\Sigma_t^\epsilon$. In this way, R coincides with the radius of $\tilde\Sigma_t^\epsilon$. The surface $\tilde\Sigma_t^\epsilon$ translates along the z-axis as $r(t) \to 0$. Ultimately, we would like Σ_t^ϵ to be an open sphere of radius R whose center is stationary. To do so, we translate the previous coordinate system so that the base of the sphere lies at the origin and define, for $\tilde\zeta > 0$,

$$\frac{z}{r} = \frac{\sin\tilde\zeta}{\cosh\lambda - \cos\tilde\zeta} + \frac{\sin\zeta}{1+\cos\zeta}, \quad \frac{\varpi}{r} = \frac{\sinh\lambda}{\cosh\lambda - \cos\zeta}. \tag{26}$$

Let Σ_t^ϵ be the locus of points $(z(\lambda), \varpi(\lambda), \phi)$ from (26) for $0 \le \lambda < \infty$, $\tilde\zeta = \zeta$, and $0 \le \phi < 2\pi$ as depicted in Figure 3. By introducing $\tilde\zeta$ in (26), we generate a curve $(z(\tilde\zeta), \varpi(\tilde\zeta))$ orthogonal

to the section of Σ_t^ϵ. This gives a convenient way to compute the normal derivative needed shortly. Define the tangential velocity

$$v_s(\lambda) = \frac{r'}{\cos\zeta}\sqrt{\frac{\cosh\lambda - 1}{\cosh\lambda + 1}} \tag{27}$$

and normal velocity

$$v_n(\lambda) = 0.$$

With this velocity, the rim of the hole contracts with rate r' and the area density of the surface is independent of position (but not time). A short calculation verifies that $v_s(0) = 0$, $\lim_{\lambda\to\infty} v_s(\lambda) = \frac{r'}{\cos\zeta}$, and that v_s is a solution to (6). Also, the radial plug flow is recovered in the limit

$$\lim_{\epsilon\to 0} v_s = r'\frac{r}{\varpi}\Big|_{\epsilon=0},$$

as required by (15).

Consider the creeping flow boundary value problem associated with the bounding region Σ_t^ϵ;

$$D^2\psi^\epsilon = 0, \quad x \in \mathbb{R}^3 \setminus \Sigma_t^\epsilon, \tag{28}$$

$$\frac{1}{\varpi}\frac{\partial\psi^\epsilon}{\partial s} = 0, \quad x \in \Sigma_t^\epsilon, \tag{29}$$

$$\frac{1}{\varpi}\frac{\partial\psi^\epsilon}{\partial n} = v_s, \quad x \in \Sigma_t^\epsilon, \tag{30}$$

$$\psi^\epsilon = 0, \quad \varpi = 0. \tag{31}$$

To solve the boundary value problem (28-31) by the method of perturbation expansion, we tentatively assume that a perturbation expansion

$$\psi^\epsilon(p,q,t;\epsilon) = \psi^0(p,q,t) + \epsilon\psi^1(p,q,t) + \dots \tag{32}$$

holds in a neighborhood of $\epsilon = 0$. The general strategy is to substitute this expansion into the equations (28-31). Equating like powers in ϵ allows a determination of ψ^0 and ψ^1 as

solutions to auxiliary boundary value problems. Noting that $\psi = 0$ on the intersection of Σ_t^ϵ with the axis of symmetry, (29) implies that

$$\psi^0 + \epsilon\psi^1 + \cdots = 0, \quad x \in \Sigma_t^\epsilon.$$

Here, p and q depend implicitly on ϵ, necessitating an expansion of ψ^0 and ψ^1 before equating like powers. We do so by fixing λ, and allowing a given point on Σ_t^ϵ to approach the plane as $\epsilon \to 0$. With the help of (10) and (26), expanding into a Taylor series in ϵ, using the chain rule and the fact that $q_\epsilon = 0$ and $p_\epsilon = \frac{q}{2} + \frac{1}{2q}$, we find that

$$\psi^0 + \epsilon\left(\psi^1 + \left(\frac{q}{2} + \frac{1}{2q}\right)\psi_p^0\right) + \cdots = 0. \tag{33}$$

The subscripts p, q, and ϵ refer to their respective partial derivatives evaluated at $\epsilon = \zeta = 0$ and fixed λ. Similarly, the condition (30) implies that

$$\frac{\partial\psi^0}{\partial n} + \epsilon\frac{\partial\psi^1}{\partial n} + \cdots = \varpi v_s, \quad x \in \Sigma_t^\epsilon. \tag{34}$$

To equate like powers, we rewrite the normal derivative in terms of the partial derivatives in p and q and then expand each term appearing in the chain rule in terms of ϵ. Fixing ϵ and allowing $\tilde{\epsilon}$ to vary in (26) we find, after some calculation,

$$\frac{\partial}{\partial n} = \mathscr{P}\frac{\partial}{\partial p} + \mathscr{Q}\frac{\partial}{\partial q} \tag{35}$$

where $\mathscr{P}$ and $\mathscr{Q}$ satisfy

$$\mathscr{P}|_{\epsilon=0} = \frac{1}{rq}, \quad \mathscr{P}_\epsilon = 0, \quad \mathscr{Q}|_{\epsilon=0} = 0, \quad \mathscr{Q}_\epsilon = \frac{1-q^4}{2rq^3}.$$

Also, $\varpi v_s|_{\epsilon=0} = rr'$ and $(\varpi v_s)_\epsilon = 0$. With the help of (35), expanding (34) in powers of ϵ gives

$$\begin{aligned} r'r &= \mathscr{P}\psi_p^0 + \mathscr{Q}\psi_q^0 + \epsilon(\mathscr{P}\psi_p^1 + \mathscr{Q}\psi_q^1 + \mathscr{P}_\epsilon\psi_p^0 + \mathscr{P}\psi_{pp}^0 p_\epsilon + \mathscr{Q}_\epsilon\psi_q^0 + \mathscr{Q}\psi_{qq}^0 q_\epsilon) + \cdots \\ &= \frac{1}{rq}\psi_p^0 + \epsilon\left(\frac{1}{rq}\psi_p^1 + \frac{1}{rq}\left(\frac{q}{2} + \frac{1}{2q}\right)\psi_{pp}^0 + \frac{1-q^4}{2rq^3}\psi_q^0\right) + \cdots . \end{aligned} \tag{36}$$

Consolidating the results from (33) and (36) yields

$$\psi^0(1,q) = 0, \quad \psi^0(0,q) = 0, \quad \psi_p^0(0,q) = r'r^2q, \quad -\infty < q < \infty,$$

and

$$\psi^1(1,q)=0,\quad \psi^1(0,q)=-\left(\frac{q}{2}+\frac{1}{2q}\right)\psi^0_p,\quad \psi^1_p(0,q)=-\left(\frac{q}{2}+\frac{1}{2q}\right)\psi^0_{pp}-\frac{1-q^4}{2q^2}\psi^0_q$$

for $-\infty<q<\infty$. As expected, the first three of the previous six equations are the same as (20) that appeared for the stream function on the infinite, flat plane in Section 4. We identify $\psi^0=r'r^2qp(1-p)$ as before. Plugging the known value of ψ^0 into the boundary values for ψ^1 now gives

$$\psi^1(1,q)=0,\quad \psi^1(0,q)=-\frac{1}{2}r'r^2(q^2+1),\quad \psi^1_p(0,q)=r'r^2(q^2+1),\quad -\infty<q<\infty.$$

Equating these boundary values with the decomposition (14) (with $\psi_0=qp^2$ and $\psi_1=pq^2$) gives the system of equations

$$\begin{aligned}
&\frac{B_1}{6}q^3+\left(B'+\frac{B_2}{2}+\frac{B_0}{2}\right)q^2+\left(A_3+B_1+B-\frac{B_1}{2}\right)q+A_0+A_1-\frac{B_2}{6}+\frac{B_0}{2}=0,\\
&\frac{B_1}{6}q^3+\left(\frac{B_0}{2}-\frac{A_4}{4}\right)q^2+B_1q+B_0+A_0-\frac{A_4}{4}=-\frac{1}{2}r'r^2(q^2+1),\\
&\left(B'+\frac{B_2}{2}\right)q^2+A_3q+A_1=r'r^2(q^2+1).
\end{aligned}$$

This system has as a solution $B':A_1:B_2:A_0:A_4:B_0=(-2:1:6:1:-2:-2)r'r^2$ and all other coefficients zero. In this way

$$\begin{aligned}
\psi^\epsilon&=\psi^0+\epsilon\psi^1+\cdots\\
&=r'r^2\left[qp(1-p)+\epsilon\left(-2\psi_1+\psi_{\mathrm{irr},1}+6\psi_{\mathrm{rot},2}+\psi_{\mathrm{irr},0}-2\psi_{\mathrm{irr},4}-2\psi_{\mathrm{rot},0}\right)\right]+\cdots.
\end{aligned}\tag{37}$$

Recalling that D applied to the irrotational components of ψ^1 gives zero, we find

$$D\psi^\epsilon=r'\left[\frac{-2q(1-p^2)}{p^2+q^2}+\epsilon\left(\frac{-4p(1+q^2)}{p^2+q^2}+6p-2\right)\right]+\cdots \tag{38}$$

We evaluate (7) for the perturbation solution (37). The only technical difficulty presented by this perturbation expansion is that the integrand of order ϵ must be integrated over Σ^ϵ_t before taking the limit $\epsilon\to 0$ to avoid a divergent integral. From (37) and (38), with the

substitution $u = \cosh\lambda$, we have $dA = \frac{2\pi r\varpi}{(u-\cos\zeta)\sqrt{u^2-1}}du$ and

$$\begin{aligned}\Delta_{\mathrm{a}} &= -2\mu\int_{\Sigma_t}\frac{v_s}{\varpi}D\psi^{\epsilon}\,dA = -4\pi\mu rr'\int_1^{\infty}\frac{D\psi^{\epsilon}}{(u+1)(u-\cos\zeta)}\,du\\ &= 8\pi\mu r(r')^2\int_1^{\infty}\frac{1}{\sqrt{2}\sqrt{u-1}(u+1)}+\frac{\epsilon}{(u+1)(u-\cos\zeta)}\,du+\cdots\\ &= 8\pi\mu r(r')^2\left(\frac{\pi}{2}-\frac{\epsilon}{1+\cos\zeta}\ln\frac{1-\cos\zeta}{2}\right)+\cdots.\end{aligned}$$

Finally, using the asymptotic relationship $1-\cos\zeta = \frac{\epsilon^2}{2}+\cdots$ yields the aqueous friction and dissipation terms for a sphere with $R \gg r$;

$$\Delta_{\mathrm{a}} = 2\pi\mu r(r')^2\left(2\pi-4\epsilon\ln\frac{\epsilon}{2}+\cdots\right),\quad \mathscr{F}_{\mathrm{a}} = 2\pi\mu rr'\gamma(\epsilon),\quad \gamma(\epsilon) = 2\pi-4\epsilon\ln\frac{\epsilon}{2}+\cdots.$$

In the next section we make a comparison between pore dynamics using the value $\gamma(\epsilon)$ and the experimental record for spherical liposomes.

6 Experimental Validation

We now compare the drag coefficient $\gamma(\epsilon)$ derived by purely theoretical reasoning with the drag coefficient C derived in [20] from experimental data, which assumed that C was independent of liposome radius and hole size. Curve fitting the data with a friction term of the form $C\mu rr'$ yielded $C = 8.16$. In the experiments, the smallest measured hole radius was $r = 2$ μm and the widest measured radius was 10 μm, placing r in the range from one tenth to one half of the liposome radius, $R = 19.7$ nm. For this range of values of ϵ, the friction coefficient $\gamma(\epsilon)$ takes values between 7.4815 and 9.0558. Thus the experimental fit is in accord with the present theoretical determinations. We now use the theoretically derived coefficient $\gamma(\epsilon)$ instead of the value of the coefficient C, previously derived by curve fitting experimental data, to calculate the expected pore dynamics predicted by the theory in [20]. The agreement between the theory and experimental data is excellent. (Figure 4.)

To further validate (25) by experimental means, a single planar bilayer with diameter greater than a millimeter, could be used. For planar bilayers, surface tension σ is constant (and maintained by the supporting circular Gibbs-Plateau border of radius r_B), and the

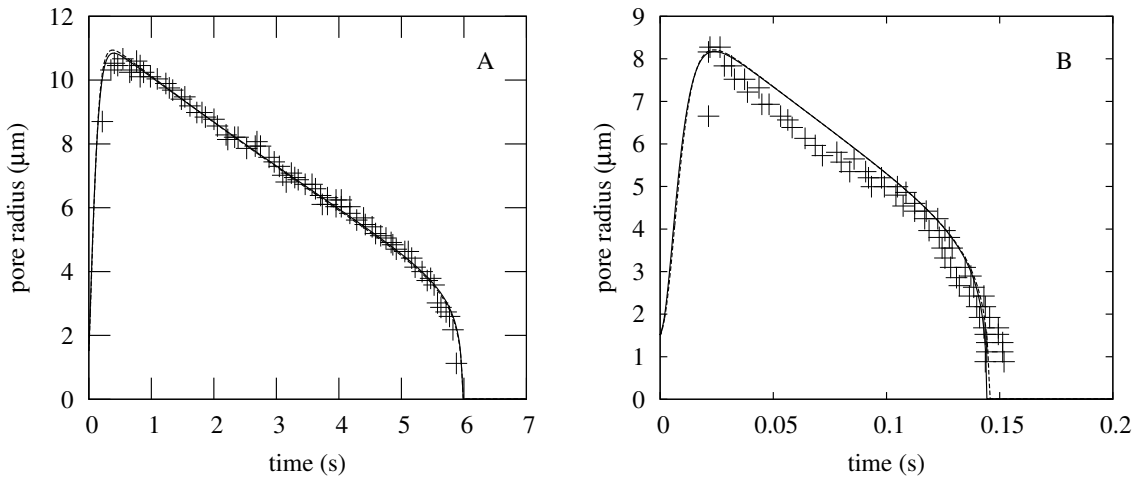

Figure 4: Comparison of the theoretically derived coefficient $\gamma(\epsilon)$ (solid lines), the experimentally inferred coefficient $C = 8.16$ (dashed lines), and the experimental record (crosses) for pore dynamics [20]. (A) For the simulation we used $\mu_0 = 32$ cP, $R = 19.7$, $\mu_l = 1$ P, $T = 12.5$ pN and $S = 0.045$ kT nm^{-2}, the values reported for the experimental records, [2] and [12]. (B) For this experimental record, aqueous viscosity was smaller $\mu_0 = 1.13$ cP ([16]) than in the record of panel A and pore dynamics is faster, underscoring the importance of aqueous viscosity. We calculated the expected pore dynamics by using the values of the physical parameters given in the experimental study: $R = 21.1$, $\mu_l = 1$ P, $T = 14$ pN and $S = 0.045$ kT nm^{-2}. As a practical matter, the curve fit value of $C = 8.16$ gives virtually the same curve as that derived using $\gamma(\epsilon)$ derived from first principles.

radial plug flow profile is undisturbed by the far field conditions. The bilayer can be punctured (e.g., by electroporation [19]) and the expansion of the hole's radius $r(t)$ measured as a function of time. The energy of the bilayer is $E = \sigma\pi(r_B^2 - r^2)$ while the aqueous dissipation of energy, according to (24), is $\Delta_{\rm a} = 4\pi^2\mu r(r')^2$. The dissipation due to bilayer friction is $\Delta_{\rm m} = 4\pi\mu_{\rm l}h(r')^2$ where h is the thickness of the bilayer (3–4 nm) and $\mu_{\rm l}$ is the viscosity of lipid [2]. Note that the aqueous dissipation, which is volumetric, is proportional to pore radius while the membrane dissipation, accounted for only in the membrane surface, is independent of this radius.

Using the Rayleigh dissipation equation, the evolution equation for the expansion of the

hole's radius in terms of the sum of the aqueous ($\gamma(0) = 2\pi$) and membrane friction is:

$$\frac{\mathscr{F}_{\mathrm{a}} + \mathscr{F}_{\mathrm{m}}}{2\pi} = (2\pi\mu r + 2h\mu_l)r' = \sigma r.$$

For moderate values of lipid viscosity ($\mu_l = 1$ P) and r in the μm range, the aqueous component of friction is dominant. In this case we predict that the settling velocity will be

$$r' = \frac{\sigma}{2\pi\mu}.$$

If, however, the contribution of the lipid viscosity μ_l to energy dissipation is high ($\mu_l \gg 1$ P), then $r(t)$ will not grow linearly but satisfy

$$2\pi\mu(r - r_0) + 2h\mu_l \ln\frac{r}{r_0} = \sigma t$$

where $r_0 = r(0)$ is the radius directly after pore formation. Because the functional forms of aqueous and lipid viscosity to the time course of pore size are quite different from each other, the relative contributions of each can be determined. Prior investigators [1, 7] have established the functional form of pore growth in the extreme case of a lipid film suspended in air. Because aqueous friction is zero in this case, pore dynamics is affected by membrane friction alone.

7 Conclusion

Experiments that measure the expansion and contraction of holes in liposomes motivated us to formulate a boundary value problem to determine the motion of an incompressible, viscous fluid surrounding a spherical surface of zero thickness when a hole in the surface expands or contracts with a prescribed velocity. The analogue of radial plug flow for a spherical shape was derived under the assumption that the surface density is spatially constant. This allowed us to derive a stream function using a perturbation expansion and then calculate the dissipation function for the flow field.

The zeroth order term in the stream function perturbation expansion is an exact solution to the Stokes system. One can take advantage of the closed form expression by considering

other perturbation problems where the limiting shape is similar to the plane region studied here. Alternatively, since the surface velocity is known, the flow field can be determined from the Green's function representation used by the boundary integral method. Although mathematically more complicated, not only could the velocity expressions be derived, but the error of the perturbation solution as a function of the perturbation parameter could be estimated.

8 Appendix

By performing a separation of variables to the equation $D\psi = 0$, we express the irrotational stream functions in terms of $(I_n(p), H_n(p))$ $(J_n(q), G_n(q))$, $n = 0, 1, 2, \ldots$ where I_n and H_n form the solution set for

$$(1 - p^2)P'' + n(n-1)P = 0,$$

and where J_n and G_n form the solution set for

$$(1 + q^2)Q'' - n(n-1)Q = 0.$$

The Gegenbauer functions I_n and H_n satisfy

$$\begin{aligned} I_n(p) &= \frac{1}{(n-1)!}\left(\frac{d}{dp}\right)^{n-2}\left(\frac{p^2-1}{2}\right)^{n-1}, \quad n = 2, 3, \ldots, \\ H_n(p) &= \frac{1}{2}I_n(p)\ln\frac{p+1}{p-1} - K_n(p), \qquad\qquad n = 2, 3, \ldots, \end{aligned}$$

where $K_n(p)$ are polynomial. For the exceptional cases $n = 0, 1$ we define $I_0(p) = -1$, $H_0(p) = p$, $I_1(p) = p$, and $H_1(p) = -1$ and set $I_m(p) = H_m(p) = 0$ for $m = -2, -1$. The functions $J_n(q)$ and $G_n(q)$ are obtained by setting

$$i^n J_n(q) = I_n(iq), \quad i^{n+1}G_n(q) = H_n(iq), \quad n = -2, -1, 0, \ldots$$

The functions $I_n(p)$ and $J_n(q)$ are polynomials. For $n = 2, 3, \ldots$, the functions $H_n(p)$ are singular at $p = 1$ and the functions $G_n(q)$ are discontinuous at $q = 0$. For this reason we retain

only H_0, H_1, G_0, G_1, and I_n and J_n for $n = 0, 1, 2, \ldots$ in the series expansion of physically realizable stream functions and deem the functions H_n and G_n for $n = 2, 3, \ldots$ unphysical. The functions (12) are obtained by forming the products of $(I_0(p), H_0(p))$, $(I_1(p), H_1(p))$, and $I_n(p)$, $n = 2, 3, \ldots$ with $(J_0(p), G_0(p))$, $(J_1(p), G_1(p))$, and $J_n(p)$, $n = 2, 3, \ldots$ respectively. The rotational components (13) are now found by setting $\psi_{\text{rot},1} = \frac{1}{2}q\left(\frac{1}{3}q^2 - p^2\right)$, $\psi_{\text{rot},2} = \frac{1}{2}p\left(q^2 - \frac{1}{3}p^2\right)$, and with the help of the identity ([23])

$$p^2 I_n(p) = \delta_n I_{n+2}(p) + \epsilon_n I_n(p) + \zeta_n I_{n-2}(p), \quad n = 0, 1, 2, \ldots,$$

for the values $\delta_n = \frac{(n+1)(n+2)}{(2n-1)(2n+1)}$, $\epsilon_n = \frac{2n^2-2n-3}{(2n+1)(2n-3)}$, and $\zeta_n = \frac{(n-2)(n-3)}{(2n-1)(2n-3)}$.

References

[1] M. Brenner and D. Gueyffier. On the bursting of viscous films. *Phys. Fluids*, 11(3):737–739, 1999.

[2] F. Brochard, P. G. de Gennes, and O. Sandre. Transient pores in stretched vesicles: role of leakout. *Physica A*, 278(1-2):32–51, 2000.

[3] G. F. Carrier and C. C. Lin. On the nature of the boundary layer near the leading edge of a flat plate. *Quarterly of Applied Mathematics*, VI(1):63–68, 1948.

[4] K. Dalnoki-Veress, B. G. Nickel, C. Roth, and J. R. Dutcher. Hole formation and growth in freely standing polystyrene films. *Physical Review E*, 59(2):2153–2156, 1999.

[5] A. M. J. Davis. Shear flow disturbance due to a hole in the plane. *Physics of Fluids A.*, 3(3):478–480, 1991.

[6] G. Debrégeas, G. P. de Gennes, and F. Brochard-Wyart. The life and death of viscous "bare" bubbles. *Science*, 279:1704–1707, 1999.

[7] G. Debrégeas, P. Martin, and F. Brochard-Wyart. Viscous bursting of suspended films. *Physical Review Letters*, 75, 1995.

[8] J.M. Dorrepaal, M. E. O'Neill, and K. B. Ranger. Axisymmetric stokes flow past a spherical cap. *J. Fluid Mech.*, 75:273–286, 1976.

[9] T. Fang and H. Tao. Unsteady viscous flow over a rotating stretchable disk with deceleration. *Communications in Nonlinear Science and Numerical Simulation*, 17(17):5064–5072, 2012.

[10] Roland Glowinski. *Finite element methods for incompressible viscous flow.* Volume IX. North-Holland, Amsterdam, 2003.

[11] John Happel and Howard Brenner. *Low Reynolds number hydrodynamics with special applications to particulate media.* Prentice-Hall Inc., Englewood Cliffs, N.J., 1965.

[12] E. Karatekin, O. Sandre, H. Guitouni, N. Borghi, P. H. Puech, and F. Brochard-Wyart. Cascades of transient pores in giant vesicles: Line tension and transport. *Biophys J.*, 84, 2003.

[13] C. J. Lawrence and S. Weinbaum. The unsteady force on a body at low reynolds number; the axisymmetric motion of a spheroid. *J. Fluid Mech.*, 189:463–489, 1989.

[14] J. S. Lowengrub, J.-J. Xu, and A. Voigt. Surface phase separation and flow in a simple model of multicomponent drops and vesicles. *Fluid Dynamics and Materials Processing*, 3(1):1–19, 2007.

[15] C. Peskin. The immersed boundary method. *Acta Numerica*, 11:479–517, 2002.

[16] T. Portet and R. Dimova. A new method for measuring edge tension and stability of lipid bilayers: Effect of membrane composition. *Biophys J.*, 99:3264–3273, 2010.

[17] C. Pozrikidis. *Boundary integral and singularity methods for linearized viscous flow.* Cambridge Texts in Applied Mathematics. Cambridge University Press, Cambridge, 1992.

[18] K. B. Ranger. The stokes drag for asymmetric flow past a spherical cap. *Zeitschrift Für Angewendete Mathematik und Physik*, 24:801–809, 1973.

[19] K. A. Riske and R. Dimova. Electro-deformation and poration of giant vesicles viewed with high temporal resolution. *Biophys J.*, 88:1143–1155, 2005.

[20] R. J. Ryham, I. Berezovik, and F. S. Cohen. Aqueous viscosity is the primary source of friction in lipidic pore dynamics. *Biophys J.*, 101(12):2929–2938, 2011.

[21] R. J. Ryham, F. S. Cohen, and R. S. Eisenberg. A dynamic model of open vesicles in fluids. *Communications in Mathematical Sciences*, 10(4):1273–1285, 2012.

[22] J. E. Sader. Frequency response of cantilever beams immersed in viscous fluids with applications to the atomic force microscope. *Journal of Applied Physics*, 84:64–76, 1998.

[23] R. A. Sampson. On Stokes' current function. *Phil. Trans. R. Soc. Lond. A*, 182:449–518, 1891.

[24] N. Savva and J. W. M. Bush. Viscous sheet retraction. *J. Fluid Mech.*, 626:211–240, 2009.

[25] J. Sohn, Y.-H. Tseng, S. Li, A. Voigt, and J. Lowengrub. Dynamics of multicomponent vesicles in a viscous fluid. *Journal of Computational Physics*, 229(1):119–144, 2010.

[26] Milton Van Dyke. *Perturbation methods in fluid mechanics*. The Parabolic Press, Stanford, Calif., annotated edition, 1975.

[27] P. M. Vlahovska, Y.-N. Young, G. Danker, and C. Misbah. Dynamics of a non-spherical microcapsule with incompressible interface in shear flow. *J. Fluid Mechanics*, 678:221–247, 2011.